Acta Cryst E CRYSTALLOGRAPHIC COMMUNICATIONS

ISSN 2056-9890

Crystal structure and Hirshfeld surface analysis of 2-azido-*N*-(4-fluorophenyl)acetamide

Mohcine Missioui,[a] Walid Guerrab,[a] Abdulsalam Alsubari,[b]* Joel T. Mague[c] and Youssef Ramli[a]‡

[a]Laboratory of Medicinal Chemistry, Drug Sciences Research Center, Faculty of Medicine and Pharmacy, Mohammed V University in Rabat, Morocco, [b]Laboratory of Medicinal Chemistry, Faculty of Clinical Pharmacy, 21 September University, Yemen, and [c]Department of Chemistry, Tulane University, New Orleans, LA 70118, USA. *Correspondence e-mail: alsubaripharmaco@21umas.edu.ye

Received 6 June 2022
Accepted 30 June 2022

Edited by L. Van Meervelt, Katholieke Universiteit Leuven, Belgium

‡ Additional correspondence author, e-mail: y.ramli@um5r.ac.ma.

Keywords: crystal structure; azide; acetamide; hydrogen bond; Hirshfeld surface.

CCDC reference: 2183049

Supporting information: this article has supporting information at journals.iucr.org/e

The asymmetric unit of the title compound, $C_8H_7FN_4O$, consists of two independent molecules differing in the orientation of the azido group. Each molecule forms N—H···O hydrogen-bonded chains along along the *c*-axis direction with its symmetry-related counterparts and the chains are connected by C—F···π(ring), C═O···π(ring) and slipped π-stacking interactions. A Hirshfeld surface analysis of these interactions was performed.

1. Chemical context

Azides are a class of versatile organic compounds having the basic structure RN_3 where *R* can be an alkyl, acyl or aryl group. They have found valuable applications in medicinal chemistry (Contin *et al.*, 2019) and molecular biology (Ahmed & Abdallah, 2019). On the other hand, amide bonds are a key structural unit in many physiologically active compounds and have ubiquitous presence in biopolymers such as proteins and glycoproteins (Cheng *et al.*, 2016; Pattabiraman & Bode, 2011; Zheng *et al.*, 2016). Acetamides are useful building blocks for the preparation of biologically active natural products, especially depsipeptide compounds. In particular, *N*-arylacetamides are significant intermediates for the synthesis of medicinal, agrochemical, and pharmaceutical compounds (Valeur & Bradley, 2009; Allen & Williams, 2011; Missioui *et al.*, 2021; Missioui *et al.*, 2022*a*,*b*). They have been identified as inhibitors of methionine aminopeptidase-2 and HIV protease, display potent antitumor activity, and play an important role in medicinal chemistry. As a result of the significance of this core, and in a continuation of our research efforts to synthesize *N*-arylacetamide-based heterocycles (Missioui *et al.*, 2020; Al-Taifi *et al.*, 2021; Guerrab *et al.*, 2021; Missioui *et al.*, 2022*c*,*d*), we report here the synthesis, molecular and crystal structures and a Hirshfeld surface analysis of the title compound.

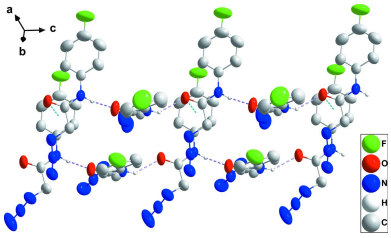

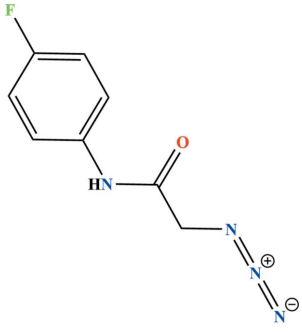

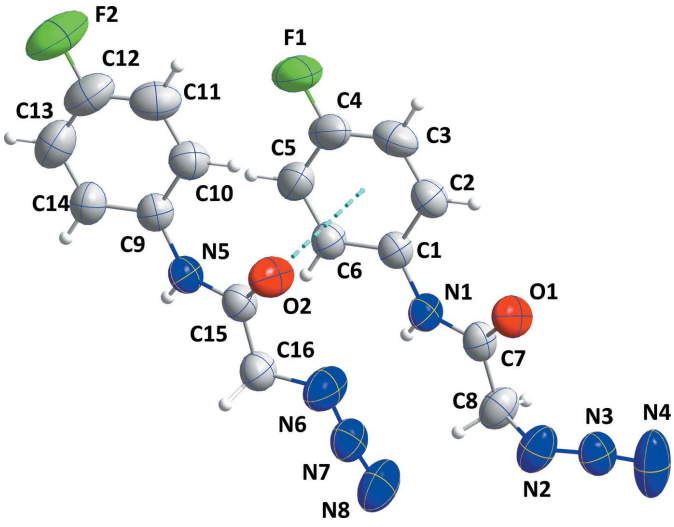

Figure 1
The asymmetric unit with labeling scheme and 50% probability ellipsoids. The C15═O2···*Cg*1 interaction is depicted by a dashed line.

2. Structural commentary

The asymmetric unit consists of two independent molecules differing moderately in conformation and connected by a weak C15═O2···*Cg*1 interaction [*Cg*1 is the centroid of the C1–C6 benzene ring; O2···*Cg*1 = 3.904 (2) Å, C15···*Cg*1 = 3.902 (2) Å, C15═O2···*Cg*1 = 80.88 (13)°] as shown in Fig. 1. The conformational difference is primarily in the orientation of the azide groups (Fig. 2). Thus the N3—N2—C8–C7 torsion angle between the planes defined by N1/C7/C8/O1 and C8/N2/N3/N4 is −106.1 (2)° while the corresponding dihedral angle in the other molecule is −175.4 (2)°. The dihedral angle between the plane defined by N1/C7/C8/O1 and that of the C1-C6 ring is 21.85 (13)° while the corresponding angle (N7—N6—C16—C15) in the other molecule is the same within experimental error. By comparison, in the *p*-tolyl analog (Missioui *et al.*, 2022*e*), which has three independent molecules in the asymmetric unit, the dihedral angles between the N/C/C/O and C/N/N/N planes are 7.6 (2), 86.34 (19) and 7.03 (19)° while those between the N/C/C/O and phenyl ring planes are 24.2 (2), 22.58 (10) and 15.38 (10)°.

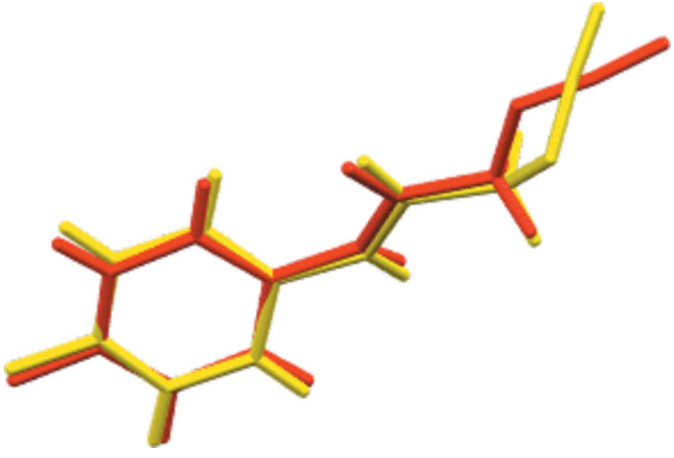

Figure 2
Overlay of the two molecules in the asymmetric unit. The yellow molecule contains O1 while the red one contains O2.

Table 1
Hydrogen-bond geometry (Å, °).

*Cg*1 and *Cg*2 are the centroids of the C1–C6 and C9–C14 benzene rings, respectively.

D—H···*A*	*D*—H	H···*A*	*D*···*A*	*D*—H···*A*
N1—H1···O1^{i}	0.86	2.17	2.921 (2)	146
N5—H5*A*···O2^{i}	0.86	2.13	2.885 (2)	146
C4—F1···*Cg*1^{ii}	1.35 (1)	3.76 (1)	3.563 (2)	72 (1)
C12—F2···*Cg*2^{iii}	1.36 (1)	3.98 (1)	3.942 (2)	79 (1)

Symmetry codes: (i) $x, -y+\frac{1}{2}, z+\frac{1}{2}$; (ii) $-x+1, -y+1, -z+1$; (iii) $-x+2, -y+1, -z+2$.

3. Supramolecular features

In the crystal, the molecule containing O1 is linked into chains extending along the *c*-axis direction by N1—H1···O1^{i} hydrogen bonds [symmetry code: (i) $x, -y+\frac{1}{2}, z+\frac{1}{2}$], while N5—H5*A*···O2^{i} hydrogen bonds form parallel chains for the second independent molecule (Table 1 and Fig. 3). The chains are linked by C4—F1···*Cg*1^{ii} and C12—F2···*Cg*2^{iii} [*Cg*2 is the centroid of the C9–C14 benzene ring; symmetry codes: (ii) $-x+1, -y+1, -z+1$; (iii) $-x+2, -y+1, -z+2$] interactions as well as by the C15═O2···*Cg*1 interaction noted above and weak, slipped π-stacking between centrosymmetrically related C1–C6 benzene rings [centroid–centroid = 3.8661 (13) Å, slippage = 1.6 Å] (Table 1 and Fig. 4). For the related *p*-tolyl analog (Missioui *et al.*, 2022*e*) each independent molecule forms chains with its symmetry-related counterparts through N—H···O hydrogen bonds. There do not appear to be significant intermolecular interactions between the chains although it is possible that very weak C═O···π(ring) interactions exist.

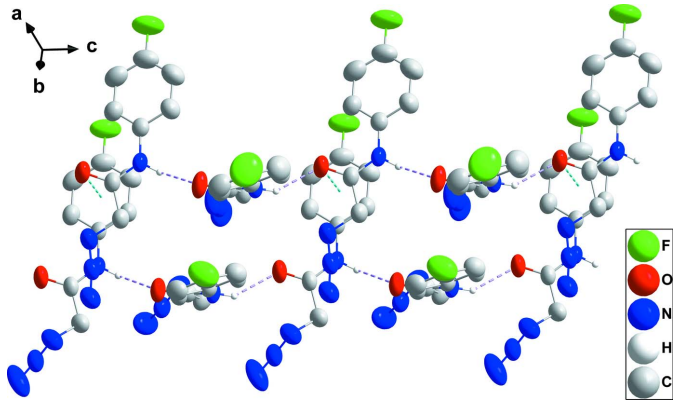

Figure 3
Perspective view of the chain structure with N—H···O hydrogen bonds and C15═O2···*Cg*1 interactions depicted, respectively, by violet and light-blue dashed lines. Non-interacting hydrogen atoms are omitted for clarity.

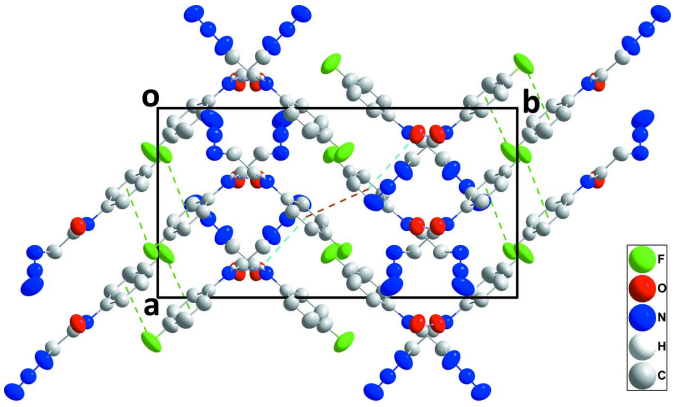

Figure 4
Packing viewed along the *c*-axis direction showing the linking of chains *via* C—F···π(ring) (green dashed lines) and C15═O2···*Cg*1 (light-blue dashed lines) and slipped π-stacking (orange dashed lines) interactions. N—H···O hydrogen bonds and non-interacting hydrogen atoms are omitted for clarity.

4. Database survey

A search of the Cambridge Structural Database (CSD, version 5.43, updated to March 2022; Groom *et al.*, 2016) with the search fragment **A** gave eleven hits of which three contained the 2-azidoacetamide unit while 30 hits resulted from a search with fragment **B**, of which six contained the 2-azidoacetamide unit.

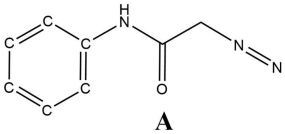

A

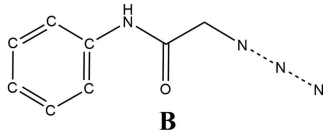

B

In the first group, the aromatic ring has a –CO_2Et group in the 2-position (ARAPIU: Yassine *et al.*, 2016*a*), the second has ^{i}PrS– groups in the 2- and 3-positions (CEMRUJ: Okamura *et al.*, 2013) and the last has a –$CO_2{}^{n}$Bu group in the 2-position (OVIBAY: Yassine *et al.*, 2016*b*). The six relevant structures in the second group include ones with an unsubstituted phenyl group (ASEDIO: Guerrab *et al.*, 2021) and those with the 4-position containing –NO_2 (QAGNOF: Missioui *et al.*, 2020), HC≡C– (DAPYOM: Madhusudhanan *et al.*, 2021), MeO– (TARHIH: Missioui *et al.*, 2021) and 2-acetoxymethyl-3,4,5-triacetoxy-tetrahydro-2*H*-pyran-6-yl-O– (BEBPIJ: Cecioni *et al.*, 2012). The sixth has Cl at the 4-position and a 2-chlorobenzoyl substituent in the 2-position (VIFVOX: Cortes Eduardo *et al.*, 2012). In ARAPIU and OVIBAY, the amide hydrogens form intramolecular N—H···O hydrogen bonds with the carboxyl oxygen while in CEMRUJ an intramolecular interaction of the amide hydrogen with the sulfur atom in the 2-position is postulated. Thus, none of these structures show the formation of chains as seen in the present case nor do any have more than one molecule in the asymmetric unit. Among the others, ASEDIO has two independent molecules in the asymmetric unit and it also, like QAGNOF and BEBPIJ, forms chains through N—H···O hydrogen bonds. In ASEDIO, the chains are connected by π-interactions between the terminal two nitrogens of the azide group and a phenyl ring, while in QAGNOF the chains are connected by C—H···O and C—H···N hydrogen bonds. The remaining structures in the first group all contain the —N═N—C fragment while the remainder of the second group all contain triazoles as the N_3-containing fragment and are not considered relevant to the present structure.

5. Hirshfeld surface analysis

A Hirshfeld surface analysis was performed with *CrystalExplorer 21.5* (Spackman *et al.*, 2021) with the details of the pictorial output described in a recent publication (Tan *et al.*, 2019). Fig. 5*a* and 5*c*, respectively, show the d_{norm} surfaces of the molecule containing O1 and that containing O2 plotted over the range −0.4316 to 1.3253 in arbitrary units while Fig. 5*b* and 5*d* show the corresponding shape-index functions. In both, two adjacent molecules that are part of the hydrogen-bonded chains are included with the N—H···O and C—H···O interactions shown by dashed lines. The pattern of orange and blue triangles indicative of a π-interaction is clearly evident in the lower part of Fig. 5*b* and corresponds to the C4—F1···*Cg*1 interaction. This is less clear in Fig. 5*d* but the data in Table 1 clearly support a similar interaction for this molecule. Fig. 6 presents fingerprint plots for the molecule containing O1 with Fig. 6*a* showing all intermolecular interactions and Fig. 6*b*–6*f* those delineated into N···H/H···N (34.3%), H···H (13.5%), O···H/H···O (12.2%), C···H/H···C (11.9%) and F···H/H···F (9.7%), respectively. The two spikes in Fig. 6*d* primarily represent the N—H···O hydrogen bonds but their breadth at longer values of $d_i + d_e$ than at the

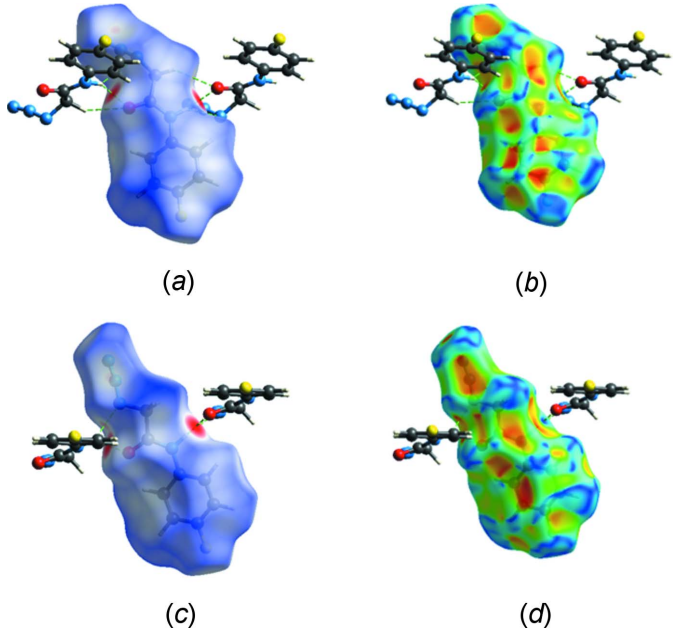

Figure 5
The (*a*) d_{norm} and (*b*) shape-index surfaces for the molecule containing O1, and the (*c*) d_{norm} and (*d*) shape-index surfaces for the molecule containing O2 together with the two closest molecules of each type.

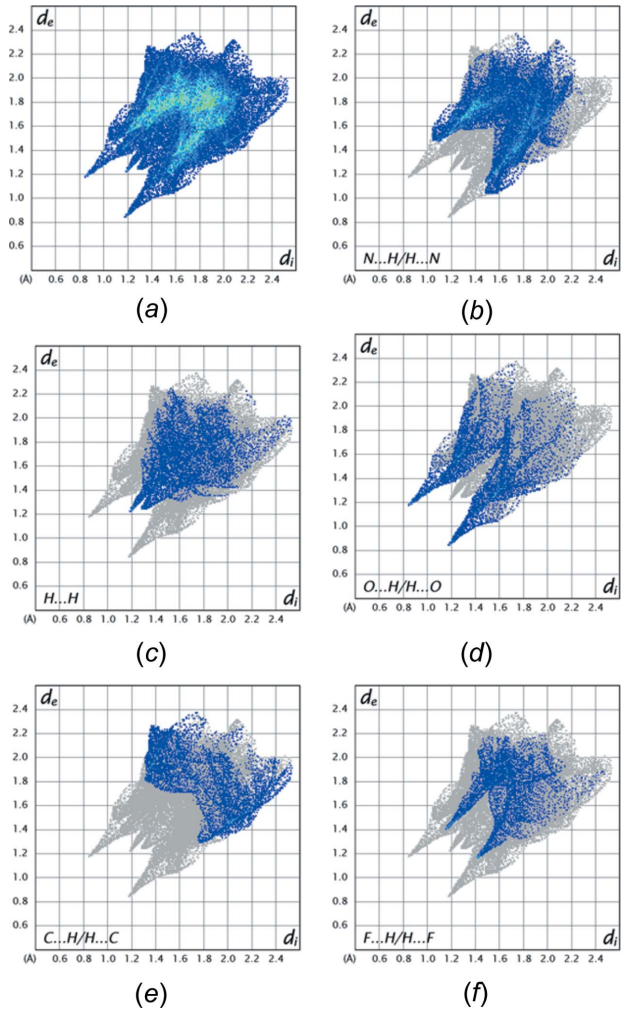

Figure 6
Fingerprint plots for the molecule containing O1 showing intermolecular interactions. (*a*) all; (*b*) N···H/H···N; (*c*) H···H; (*d*) O···H/H···O; (*e*) C···H/H···C; (*f*) F···H/H···F.

tips indicate the contributions from C—H···O hydrogen bonds. Fig. 7 shows the fingerprint plots for the molecule containing O2 with Fig. 7*a* showing all intermolecular interactions and Fig. 7*b*–7*f* those delineated into N···H/H···N (28.8%), H···H (18.2%), C···H/H···C (12.6%), F···H/H···F (12.6%) and O···H/H···O (11.6%), respectively. Although the ordering of interactions based on their percentage of the total is not the same as in the other molecule, the percentages are not greatly different between the two and the corresponding plots are very similar type by type.

6. Synthesis and crystallization

2-Chloro-*N*-(4-fluorophenyl)acetamide (0.011 mol), and sodium azide (0.015 mol) were dissolved in a mixture of ethanol/water (70:30) and refluxed for 24 h at 353 K. After completion of the reaction (monitored by thin-layer chromatography, TLC), the 2-azido-*N*-(4-fluorophenyl)acetamide that precipitated was filtered off and washed with cold water. A portion of the product was dissolved in hot ethanol, the solution was filtered, and the filtrate was left undisturbed for 7 days to form colorless, thick plate-like crystals.

Yield 69%, m.p. 358–360K, FT–IR (ATR, υ, cm^{-1}) 3254 υ (N—H amide), 1027 υ (N—C amide), 1660 υ (C═O amide), 3073 υ(C—H$_{arom}$), 1175 υ(C—N), 2961 υ(C—H, CH$_2$), 2109 υ (N$_3$), ^{1}H NMR (DMSO–d_6) δ ppm: 4.02 (2H, *s*, CH$_2$), 6.93–7.11 (4H, *m*, *J* = 1.3 Hz, H$_{arom}$), 10.05 (1H, *s*, NH), ^{13}C NMR (DMSO–d_6) δ ppm: 51.18 (CH$_2$), 131.47 (C$_{arom}$—N), 113.90–120.86 (C$_{arom}$); 165.71 (C═O); HRMS (ESI–MS) (*m*/*z*) calculated for C$_8$H$_7$FN$_4$O 194.18; found 194.1165.

7. Refinement

Crystal data, data collection and structure refinement details are summarized in Table 2. H atoms attached to carbon were placed in calculated positions (C—H = 0.95–0.99 Å) while those attached to nitrogen were placed in locations derived from a difference map and their parameters adjusted to give N—H = 0.91 Å. All were included as riding contributions with

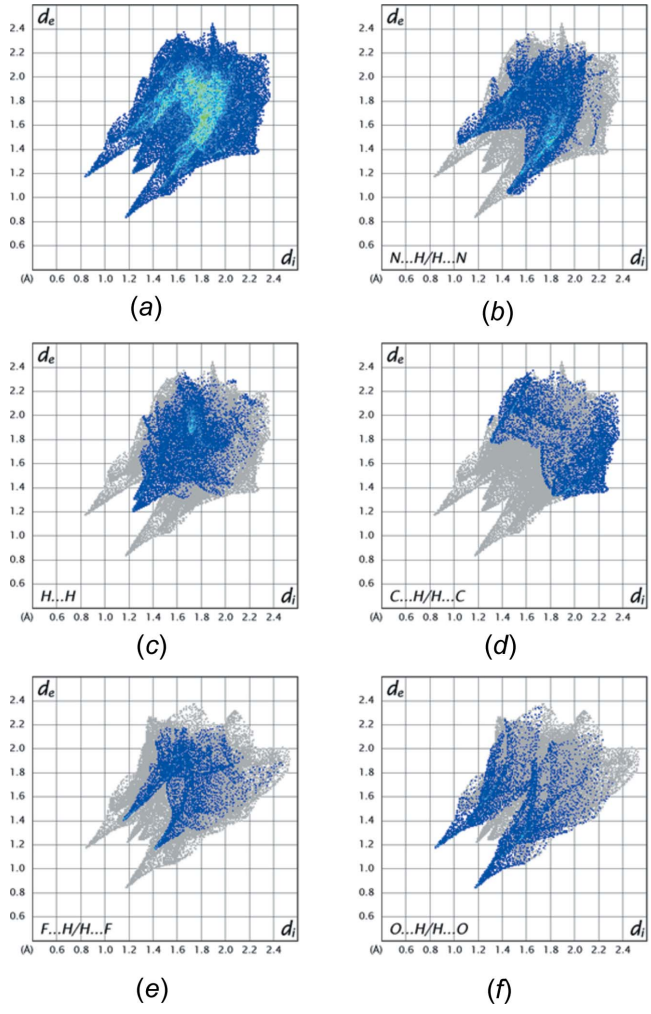

Figure 7
Fingerprint plots for the molecule containing O2 showing intermolecular interactions. (*a*) all; (*b*) N···H/H···N; (*c*) H···H; (*d*) C···H/H···C; (*e*) F···H/H···F; (*f*) O···H/H···O.

Table 2
Experimental details.

Crystal data	
Chemical formula	$C_8H_7FN_4O$
M_r	194.18
Crystal system, space group	Monoclinic, $P2_1/c$
Temperature (K)	296
a, b, c (Å)	10.8398 (7), 19.0207 (11), 9.3307 (5)
β (°)	112.378 (2)
V (Å^3)	1778.93 (18)
Z	8
Radiation type	Cu $K\alpha$
μ (mm^{-1})	1.00
Crystal size (mm)	0.47 × 0.25 × 0.15
Data collection	
Diffractometer	Bruker D8 VENTURE PHOTON 100 CMOS
Absorption correction	Multi-scan (*SADABS*; Krause *et al.*, 2015)
T_{min}, T_{max}	0.75, 0.87
No. of measured, independent and observed [$I > 2\sigma(I)$] reflections	12623, 3224, 2545
R_{int}	0.034
(sin $\theta/\lambda)_{max}$ (Å^{-1})	0.603
Refinement	
$R[F^2 > 2\sigma(F^2)]$, $wR(F^2)$, S	0.053, 0.162, 1.06
No. of reflections	3224
No. of parameters	254
H-atom treatment	H-atom parameters constrained
$\Delta\rho_{max}$, $\Delta\rho_{min}$ (e Å^{-3})	0.45, −0.24

Computer programs: *APEX3* and *SAINT* (Bruker, 2016), *SHELXT/5* (Sheldrick, 2015*a*), *SHELXL2018/3* (Sheldrick, 2015*b*), *DIAMOND* (Brandenburg & Putz, 2012), and *SHELXTL* (Sheldrick, 2008).

isotropic displacement parameters 1.2–1.5 times those of the attached atoms.

Acknowledgements

Author contributions are as follows. Conceptualization, YR; methodology, MM and AA; investigation, WG, MM; writing (original draft), JMT and YR; writing (review and editing of the manuscript), YR; formal analysis, AA and YR; supervision, YR; crystal-structure determination and validation, JTM.

Funding information

The support of NSF–MRI grant No. 1228232 for the purchase of the diffractometer and Tulane University for support of the Tulane Crystallography Laboratory are gratefully acknowledged.

References

Ahmed, S. & Abdallah, N. A. (2019). *J. Pharm. Biomed. Anal.* **165**, 357–365.
Allen, C. L. & Williams, J. M. J. (2011). *Chem. Soc. Rev.* **40**, 3405–3415.
Al-Taifi, E. A., Maraei, I. S., Bakhite, E. A., Demirtas, G., Mague, J. T., Mohamed, S. K. & Ramli, Y. (2021). *Acta Cryst.* E**77**, 121–125.
Brandenburg, K. & Putz, H. (2012). *DIAMOND*, Crystal Impact GbR, Bonn, Germany.
Bruker (2016). *APEX3*, *SAINT* and *SADABS*. Bruker AXS, Inc., Madison, Wisconsin, USA.
Cecioni, S., Praly, J.-P., Matthews, S. E., Wimmerová, M., Imberty, A. & Vidal, S. (2012). *Chem. Eur. J.* **18**, 6250–6263.
Cheng, D., Liu, J., Han, D., Zhang, G., Gao, W., Hsieh, M. H. N., Ng, N., Kasibhatla, S., Tompkins, C., Li, J., Steffy, A., Sun, F., Li, C., Seidel, H. M., Harris, J. L. & Pan, S. (2016). *ACS Med. Chem. Lett.* **7**, 676–680.
Contin, M., Sepúlveda, C., Fascio, M., Stortz, C. A., Damonte, E. B. & D'Accorso, N. B. (2019). *Bioorg. Med. Chem. Lett.* **29**, 556–559.
Cortes Eduardo, C., Simon, H., Apan Teresa, R., Camacho Antonio, N. V., Lijanova, I. & Marcos, M. (2012). *Anticancer Agents Med. Chem.* **12**, 611–618.
Groom, C. R., Bruno, I. J., Lightfoot, M. P. & Ward, S. C. (2016). *Acta Cryst.* B**72**, 171–179.
Guerrab, W., Missioui, M., Zaoui, Y., Mague, J. T. & Ramli, Y. (2021). *Z. Kristallogr. New Cryst. Struct.* **236**, 133–134.
Krause, L., Herbst-Irmer, R., Sheldrick, G. M. & Stalke, D. (2015). *J. Appl. Cryst.* **48**, 3–10.
Madhusudhanan, M. C., Balan, H., Werz, D. B. & Sureshan, K. M. (2021). *Angew. Chem. Int. Ed.* **60**, 22797–22803.
Missioui, M., Guerrab, W., Alsubari, A., Mague, J. T. & Ramli, Y. (2022*e*). *IUCrData*, **7**, x220621.
Missioui, M., Guerrab, W., Mague, J. T. & Ramli, Y. (2020). *Z. Kristallogr. New Cryst. Struct.* **235**, 1429–1430.
Missioui, M., Guerrab, W., Nchioua, I., El Moutaouakil Ala Allah, A., Kalonji Mubengayi, C., Alsubari, A., Mague, J. T. & Ramli, Y. (2022*d*). *Acta Cryst.* E**78**, 687–690.
Missioui, M., Lgaz, H., Guerrab, W., Lee, H.-G., Warad, I., Mague, J. T., Ali, I. H., Essassi, E. M. & Ramli, Y. (2022*a*). *J. Mol. Struct.* **1253**, 132132.
Missioui, M., Mortada, S., Guerrab, W., Serdaroğlu, G., Kaya, S., Mague, J. T., Essassi, E. M., Faouzi, M. E. A. & Ramli, Y. (2021). *J. Mol. Struct.* **1239**, 130484.
Missioui, M., Said, M. A., Demirtaş, G., Mague, J. T., Al-Sulami, A., Al-Kaff, N. S. & Ramli, Y. (2022*b*). *Arab. J. Chem.* **15**, 103595.
Missioui, M., Said, M. A., Demirtaş, G., Mague, J. T. & Ramli, Y. (2022*c*). *J. Mol. Struct.* **1247**, 131420.
Okamura, T., Ushijima, Y., Omi, Y. & Onitsuka, K. (2013). *Inorg. Chem.* **52**, 381–394.
Pattabiraman, V. R. & Bode, J. W. (2011). *Nature*, **480**, 471–479.
Sheldrick, G. M. (2008). *Acta Cryst.* A**64**, 112–122.
Sheldrick, G. M. (2015*a*). *Acta Cryst.* A**71**, 3–8.
Sheldrick, G. M. (2015*b*). *Acta Cryst.* C**71**, 3–8.
Spackman, P. R., Turner, M. J., McKinnon, J. J., Wolff, S. K., Grimwood, D. J., Jayatilaka, D. & Spackman, M. A. (2021). *J. Appl. Cryst.* **54**, 1006–1011.
Tan, S. L., Jotani, M. M. & Tiekink, E. R. T. (2019). *Acta Cryst.* E**75**, 308–318.
Valeur, E. & Bradley, M. (2009). *Chem. Soc. Rev.* **38**, 606–631.
Yassine, H., Hafid, A., Khouili, M., Mentre, O. & Ketatni, E. M. (2016*a*). *IUCrData*, **1**, x161155.
Yassine, H., Khouili, M., Hafid, A., Mentre, O. & Ketatni, E. M. (2016*b*). *IUCrData*, **1**, x161454.
Zheng, X., Wang, L., Wang, B., Miao, K., Xiang, K., Feng, S., Gao, L., Shen, H. C. & Yun, H. (2016). *ACS Med. Chem. Lett.* **7**, 558–562.

supporting information

Acta Cryst. (2022). E**78**, 855-859 [https://doi.org/10.1107/S2056989022006764]

Crystal structure and Hirshfeld surface analysis of 2-azido-*N*-(4-fluorophenyl)-acetamide

Mohcine Missioui, Walid Guerrab, Abdulsalam Alsubari, Joel T. Mague and Youssef Ramli

Computing details

Data collection: *APEX3* (Bruker, 2016); cell refinement: *SAINT* (Bruker, 2016); data reduction: *SAINT* (Bruker, 2016); program(s) used to solve structure: *SHELXT/5* (Sheldrick, 2015*a*); program(s) used to refine structure: *SHELXL2018/3* (Sheldrick, 2015*b*); molecular graphics: *DIAMOND* (Brandenburg & Putz, 2012); software used to prepare material for publication: *SHELXTL* (Sheldrick, 2008).

2-Azido-*N*-(4-fluorophenyl)acetamide

Crystal data

$C_8H_7FN_4O$
M_r = 194.18
Monoclinic, $P2_1/c$
a = 10.8398 (7) Å
b = 19.0207 (11) Å
c = 9.3307 (5) Å
β = 112.378 (2)°
V = 1778.93 (18) Å^3
Z = 8
$F(000)$ = 800
D_x = 1.450 Mg m^{-3}
Cu $K\alpha$ radiation, λ = 1.54178 Å
Cell parameters from 8481 reflections
θ = 2.3–68.3°
μ = 1.00 mm^{-1}
T = 296 K
Thick plate, colourless
0.47 × 0.25 × 0.15 mm

Data collection

Bruker D8 VENTURE PHOTON 100 CMOS diffractometer
Radiation source: INCOATEC IμS micro–focus source
Mirror monochromator
Detector resolution: 10.4167 pixels mm^{-1}
ω scans
Absorption correction: multi-scan (*SADABS*; Krause *et al.*, 2015)
T_{min} = 0.75, T_{max} = 0.87
12623 measured reflections
3224 independent reflections
2545 reflections with $I > 2\sigma(I)$
R_{int} = 0.034
θ_{max} = 68.5°, θ_{min} = 4.4°
h = −12→11
k = −22→22
l = −11→11

Refinement

Refinement on F^2
Least-squares matrix: full
$R[F^2 > 2\sigma(F^2)]$ = 0.053
$wR(F^2)$ = 0.162
S = 1.06
3224 reflections
254 parameters
0 restraints
Primary atom site location: dual
Secondary atom site location: difference Fourier map
Hydrogen site location: inferred from neighbouring sites
H-atom parameters constrained
$w = 1/[\sigma^2(F_o^2) + (0.0828P)^2 + 0.4718P]$ where $P = (F_o^2 + 2F_c^2)/3$
$(\Delta/\sigma)_{max} < 0.001$
$\Delta\rho_{max}$ = 0.45 e Å^{-3}

$\Delta\rho_{min}$ = −0.24 e Å^{-3}

Extinction correction: *SHELXL 2018/3* (Sheldrick, 2015*b*), $Fc^*=kFc[1+0.001xFc^2\lambda^3/\sin(2\theta)]^{-1/4}$
Extinction coefficient: 0.0033 (5)

Special details

Geometry. All esds (except the esd in the dihedral angle between two l.s. planes) are estimated using the full covariance matrix. The cell esds are taken into account individually in the estimation of esds in distances, angles and torsion angles; correlations between esds in cell parameters are only used when they are defined by crystal symmetry. An approximate (isotropic) treatment of cell esds is used for estimating esds involving l.s. planes.

Refinement. Refinement of F^2 against ALL reflections. The weighted R-factor wR and goodness of fit S are based on F^2, conventional R-factors R are based on F, with F set to zero for negative F^2. The threshold expression of $F^2 > 2\text{sigma}(F^2)$ is used only for calculating R-factors(gt) etc. and is not relevant to the choice of reflections for refinement. R-factors based on F^2 are statistically about twice as large as those based on F, and R- factors based on ALL data will be even larger. H-atoms attached to carbon were placed in calculated positions (C—H = 0.95 - 0.99 Å) while those attached to nitrogen were placed in locations derived from a difference map and their parameters adjusted to give N—H = 0.91 Å. All were included as riding contributions with isotropic displacement parameters 1.2 - 1.5 times those of the attached atoms.

Fractional atomic coordinates and isotropic or equivalent isotropic displacement parameters (Å^2)

	x	*y*	*z*	U_{iso}*/U_{eq}
F1	0.75450 (16)	0.51934 (8)	0.5506 (2)	0.1053 (6)
O1	0.37628 (16)	0.27865 (8)	0.11857 (16)	0.0704 (5)
N1	0.38854 (15)	0.30447 (8)	0.36111 (17)	0.0528 (4)
H1	0.357573	0.292390	0.429765	0.063*
N2	0.23792 (19)	0.15768 (11)	0.1118 (2)	0.0780 (6)
N3	0.1406 (2)	0.15796 (10)	−0.0097 (2)	0.0673 (5)
N4	0.0587 (3)	0.15058 (17)	−0.1238 (3)	0.1192 (11)
C1	0.48107 (18)	0.36020 (10)	0.4020 (2)	0.0494 (4)
C2	0.5065 (2)	0.40201 (11)	0.2943 (2)	0.0614 (5)
H2	0.461604	0.394037	0.188729	0.074*
C3	0.5994 (2)	0.45573 (12)	0.3457 (3)	0.0725 (6)
H3	0.617810	0.483972	0.274916	0.087*
C4	0.6637 (2)	0.46685 (11)	0.5015 (3)	0.0702 (6)
C5	0.6383 (2)	0.42787 (12)	0.6092 (3)	0.0675 (6)
H5	0.681609	0.437309	0.714400	0.081*
C6	0.54707 (19)	0.37419 (11)	0.5590 (2)	0.0569 (5)
H6	0.529166	0.346752	0.631306	0.068*
C7	0.34277 (18)	0.26790 (10)	0.2280 (2)	0.0517 (5)
C8	0.2417 (2)	0.21221 (12)	0.2228 (3)	0.0655 (6)
H8A	0.265262	0.191575	0.324847	0.079*
H8B	0.154166	0.233482	0.193244	0.079*
F2	1.2344 (2)	0.51818 (12)	0.9845 (3)	0.1438 (9)
O2	0.86230 (17)	0.27797 (9)	0.55142 (18)	0.0760 (5)
N5	0.87105 (16)	0.30220 (9)	0.79296 (17)	0.0546 (4)
H5A	0.839332	0.289670	0.860681	0.065*
N6	0.6704 (2)	0.18385 (13)	0.4918 (2)	0.0899 (7)
N7	0.5847 (2)	0.14001 (11)	0.4654 (2)	0.0670 (5)
N8	0.5019 (2)	0.10061 (15)	0.4215 (3)	0.0952 (8)

C9	0.96341 (19)	0.35814 (10)	0.8354 (2)	0.0536 (5)
C10	0.9881 (2)	0.40031 (12)	0.7283 (3)	0.0644 (5)
H10	0.943298	0.392439	0.622692	0.077*
C11	1.0801 (3)	0.45421 (14)	0.7798 (4)	0.0827 (7)
H11	1.098105	0.482845	0.709361	0.099*
C12	1.1445 (3)	0.46493 (15)	0.9364 (4)	0.0907 (8)
C13	1.1195 (3)	0.42528 (16)	1.0435 (3)	0.0904 (8)
H13	1.162906	0.434404	1.148769	0.108*
C14	1.0292 (2)	0.37163 (13)	0.9929 (3)	0.0713 (6)
H14	1.011492	0.343792	1.064795	0.086*
C15	0.82697 (19)	0.26628 (10)	0.6592 (2)	0.0539 (5)
C16	0.7313 (2)	0.20775 (12)	0.6530 (2)	0.0636 (5)
H16A	0.778421	0.169287	0.719587	0.076*
H16B	0.662987	0.224593	0.687969	0.076*

Atomic displacement parameters (Å²)

	U^{11}	U^{22}	U^{33}	U^{12}	U^{13}	U^{23}
F1	0.0904 (10)	0.0706 (9)	0.1334 (15)	−0.0264 (8)	0.0185 (10)	0.0103 (9)
O1	0.0994 (11)	0.0750 (10)	0.0495 (8)	−0.0053 (8)	0.0428 (8)	−0.0079 (7)
N1	0.0596 (9)	0.0653 (10)	0.0411 (8)	−0.0057 (7)	0.0275 (7)	−0.0050 (7)
N2	0.0694 (11)	0.0849 (14)	0.0739 (13)	0.0008 (10)	0.0208 (10)	−0.0273 (10)
N3	0.0781 (12)	0.0777 (12)	0.0517 (11)	0.0052 (9)	0.0310 (10)	−0.0057 (8)
N4	0.1118 (19)	0.160 (3)	0.0615 (14)	0.0438 (19)	0.0055 (14)	−0.0281 (15)
C1	0.0507 (10)	0.0542 (10)	0.0484 (9)	0.0043 (8)	0.0247 (8)	−0.0003 (8)
C2	0.0684 (12)	0.0663 (13)	0.0534 (11)	0.0030 (10)	0.0276 (9)	0.0079 (9)
C3	0.0763 (14)	0.0614 (13)	0.0873 (16)	0.0025 (11)	0.0396 (13)	0.0198 (11)
C4	0.0589 (12)	0.0535 (12)	0.0897 (17)	−0.0022 (9)	0.0186 (11)	0.0052 (11)
C5	0.0646 (12)	0.0637 (13)	0.0652 (13)	−0.0030 (10)	0.0146 (10)	−0.0036 (10)
C6	0.0621 (11)	0.0621 (12)	0.0484 (10)	−0.0026 (9)	0.0231 (9)	−0.0008 (8)
C7	0.0568 (10)	0.0593 (11)	0.0429 (9)	0.0079 (8)	0.0234 (8)	−0.0033 (8)
C8	0.0651 (12)	0.0739 (13)	0.0620 (12)	−0.0080 (10)	0.0292 (10)	−0.0187 (10)
F2	0.1302 (15)	0.1254 (16)	0.174 (2)	−0.0711 (13)	0.0557 (15)	−0.0489 (15)
O2	0.1083 (13)	0.0784 (10)	0.0623 (9)	−0.0201 (9)	0.0561 (9)	−0.0135 (7)
N5	0.0633 (10)	0.0632 (10)	0.0437 (8)	−0.0014 (7)	0.0276 (7)	0.0018 (7)
N6	0.1168 (17)	0.1021 (17)	0.0610 (12)	−0.0385 (14)	0.0453 (12)	−0.0225 (11)
N7	0.0765 (12)	0.0788 (12)	0.0501 (9)	−0.0018 (11)	0.0292 (9)	−0.0103 (9)
N8	0.0906 (15)	0.123 (2)	0.0712 (13)	−0.0231 (15)	0.0300 (12)	−0.0307 (13)
C9	0.0530 (10)	0.0571 (11)	0.0538 (10)	0.0049 (8)	0.0239 (8)	−0.0017 (8)
C10	0.0691 (13)	0.0655 (13)	0.0654 (13)	−0.0018 (10)	0.0334 (10)	0.0007 (10)
C11	0.0871 (17)	0.0708 (15)	0.106 (2)	−0.0101 (13)	0.0538 (16)	−0.0003 (14)
C12	0.0779 (16)	0.0806 (18)	0.112 (2)	−0.0217 (13)	0.0351 (16)	−0.0251 (16)
C13	0.0863 (17)	0.096 (2)	0.0774 (17)	−0.0134 (15)	0.0181 (14)	−0.0200 (15)
C14	0.0750 (14)	0.0762 (15)	0.0578 (12)	−0.0036 (11)	0.0201 (10)	−0.0046 (11)
C15	0.0615 (11)	0.0580 (11)	0.0472 (10)	0.0029 (8)	0.0262 (9)	0.0004 (8)
C16	0.0717 (13)	0.0722 (13)	0.0502 (11)	−0.0077 (10)	0.0270 (9)	−0.0008 (9)

Geometric parameters (Å, º)

F1—C4	1.353 (3)	F2—C12	1.358 (3)
O1—C7	1.224 (2)	O2—C15	1.225 (2)
N1—C7	1.343 (2)	N5—C15	1.341 (2)
N1—C1	1.409 (2)	N5—C9	1.411 (3)
N1—H1	0.8600	N5—H5A	0.8600
N2—N3	1.220 (3)	N6—N7	1.202 (3)
N2—C8	1.455 (3)	N6—C16	1.465 (3)
N3—N4	1.105 (3)	N7—N8	1.120 (3)
C1—C2	1.389 (3)	C9—C10	1.385 (3)
C1—C6	1.390 (3)	C9—C14	1.391 (3)
C2—C3	1.386 (3)	C10—C11	1.382 (3)
C2—H2	0.9300	C10—H10	0.9300
C3—C4	1.368 (4)	C11—C12	1.374 (4)
C3—H3	0.9300	C11—H11	0.9300
C4—C5	1.359 (3)	C12—C13	1.358 (4)
C5—C6	1.374 (3)	C13—C14	1.368 (4)
C5—H5	0.9300	C13—H13	0.9300
C6—H6	0.9300	C14—H14	0.9300
C7—C8	1.511 (3)	C15—C16	1.508 (3)
C8—H8A	0.9700	C16—H16A	0.9700
C8—H8B	0.9700	C16—H16B	0.9700
C7—N1—C1	127.90 (16)	C15—N5—C9	127.53 (16)
C7—N1—H1	116.0	C15—N5—H5A	116.2
C1—N1—H1	116.0	C9—N5—H5A	116.2
N3—N2—C8	116.02 (19)	N7—N6—C16	115.87 (19)
N4—N3—N2	171.2 (3)	N8—N7—N6	171.2 (2)
C2—C1—C6	119.27 (18)	C10—C9—C14	119.6 (2)
C2—C1—N1	123.51 (17)	C10—C9—N5	123.08 (18)
C6—C1—N1	117.20 (17)	C14—C9—N5	117.35 (18)
C3—C2—C1	119.3 (2)	C11—C10—C9	119.4 (2)
C3—C2—H2	120.3	C11—C10—H10	120.3
C1—C2—H2	120.3	C9—C10—H10	120.3
C4—C3—C2	119.4 (2)	C12—C11—C10	119.1 (3)
C4—C3—H3	120.3	C12—C11—H11	120.4
C2—C3—H3	120.3	C10—C11—H11	120.4
F1—C4—C5	118.5 (2)	C13—C12—F2	119.4 (3)
F1—C4—C3	119.0 (2)	C13—C12—C11	122.5 (2)
C5—C4—C3	122.4 (2)	F2—C12—C11	118.2 (3)
C4—C5—C6	118.4 (2)	C12—C13—C14	118.5 (3)
C4—C5—H5	120.8	C12—C13—H13	120.7
C6—C5—H5	120.8	C14—C13—H13	120.7
C5—C6—C1	121.11 (19)	C13—C14—C9	120.9 (2)
C5—C6—H6	119.4	C13—C14—H14	119.6
C1—C6—H6	119.4	C9—C14—H14	119.6
O1—C7—N1	124.23 (19)	O2—C15—N5	124.02 (19)

O1—C7—C8	122.15 (17)	O2—C15—C16	121.86 (18)
N1—C7—C8	113.61 (16)	N5—C15—C16	114.10 (16)
N2—C8—C7	110.25 (17)	N6—C16—C15	107.63 (17)
N2—C8—H8A	109.6	N6—C16—H16A	110.2
C7—C8—H8A	109.6	C15—C16—H16A	110.2
N2—C8—H8B	109.6	N6—C16—H16B	110.2
C7—C8—H8B	109.6	C15—C16—H16B	110.2
H8A—C8—H8B	108.1	H16A—C16—H16B	108.5
C7—N1—C1—C2	22.8 (3)	C15—N5—C9—C10	23.2 (3)
C7—N1—C1—C6	−158.76 (19)	C15—N5—C9—C14	−158.3 (2)
C6—C1—C2—C3	1.5 (3)	C14—C9—C10—C11	1.4 (3)
N1—C1—C2—C3	179.95 (18)	N5—C9—C10—C11	179.8 (2)
C1—C2—C3—C4	−0.4 (3)	C9—C10—C11—C12	−0.3 (4)
C2—C3—C4—F1	179.9 (2)	C10—C11—C12—C13	−1.2 (5)
C2—C3—C4—C5	−1.3 (4)	C10—C11—C12—F2	180.0 (2)
F1—C4—C5—C6	−179.38 (19)	F2—C12—C13—C14	−179.6 (3)
C3—C4—C5—C6	1.8 (4)	C11—C12—C13—C14	1.6 (5)
C4—C5—C6—C1	−0.6 (3)	C12—C13—C14—C9	−0.5 (4)
C2—C1—C6—C5	−1.0 (3)	C10—C9—C14—C13	−1.0 (4)
N1—C1—C6—C5	−179.57 (18)	N5—C9—C14—C13	−179.5 (2)
C1—N1—C7—O1	−0.3 (3)	C9—N5—C15—O2	−0.3 (3)
C1—N1—C7—C8	−178.95 (18)	C9—N5—C15—C16	178.13 (18)
N3—N2—C8—C7	−106.1 (2)	N7—N6—C16—C15	−175.4 (2)
O1—C7—C8—N2	24.7 (3)	O2—C15—C16—N6	−13.6 (3)
N1—C7—C8—N2	−156.63 (18)	N5—C15—C16—N6	168.00 (19)

Hydrogen-bond geometry (Å, º)

*Cg*1 and *Cg*2 are the centroids of the C1–C6 and C9–C14 benzene rings, respectively.

D—H···*A*	*D*—H	H···*A*	*D*···*A*	*D*—H···*A*
N1—H1···O1^{i}	0.86	2.17	2.921 (2)	146
N5—H5*A*···O2^{i}	0.86	2.13	2.885 (2)	146
C4—F1···*Cg*1^{ii}	1.35 (1)	3.76 (1)	3.563 (2)	72 (1)
C12—F2···*Cg*2^{iii}	1.36 (1)	3.98 (1)	3.942 (2)	79 (1)

Symmetry codes: (i) *x*, −*y*+1/2, *z*+1/2; (ii) −*x*+1, −*y*+1, −*z*+1; (iii) −*x*+2, −*y*+1, −*z*+2.